Promotion Of Copper On The Reduction Of Cobalt Ions In Perovskite-Type Oxides

Nguyen Tien Thao
Faculty of Chemistry, VNU University of Science, Vietnam National University-Hanoi
19 – Le Thanh Tong ST, Hoan Kiem, Hanoi, VIETNAM

Abstract

Ground $LaCo_{1-x}Cu_xO_{3-\delta}$, and mixed oxide $CuO+LaCoO_3$ were characterized by several physical means as X-ray diffraction, BET, SEM, and H_2-TPR. $LaCo_{1-x}Cu_xO_{3-\delta}$ samples show a well crystallized rhombohedral structure and uniform nanocrystalites. The substitution cobalt by copper in perovskite lattice has no significant changes in the structure, but remarkably affects the reducibility of perovskite up to x =0.3. Under hydrogen treatment, the reduction temperature of cobalt ions in $LaCo_{1-x}Cu_xO_3$, varies with the intra-lattice copper. A lower cobalt reduction temperature observed for $LaCo_{1-x}Cu_xO_{3-\delta}$ in comparison to $LaCoO_3$ produces a finely dispersed bimetal on the La_2O_3 matrix. A close distance between cobalt and copper sites in the perovskite framework facilitates the reducibility of cobalt ions and improves the metallic dispersion of metals in the reduced form.

Keywords: Nanoperovskite, promotion, intra-lattice, copper, cobaltite, LaCoCuO3, reducibility.

1. Introduction

Perovskite-type mixed oxides have the cubic structure with the general formula of ABO_3 and the space-group Pm3m-Oh [1]. In the cubic structure, cation A is at the body center while the transition-metal cations (B) occupy at the cube corners. All oxygen anions stay at the midpoint of the cube edges. Thus, both A and B positions can be partially replaced by a di- or trivalent element to produce some more complicated perovskites [1,2]. For example, La can be replaced by either Sr or Th to produce a series of $La_{1-x}Sr(Th)_xCoO_3$ perovskites which played as active catalysts for carbon dioxide hydrogenation [3] and methane oxidation [4]. Nevertheless, the replacement of the cation at A-position is much less attractive than that at B-site because the nature of cation A is usually less attractive because of inactive nature of cations A [5]. In other context, the substitution of cation B by another transition element could produce various active catalysts for many potential reaction applications [1,2,6] and/or numerous supported bimetallic catalysts after tailored reductions [1,2,7-9]. For instance, Bedel et al. [5] prepared a Fe-Co alloy after reduction of $LaFe_{0.75}Co_{0.25}O_3$ orthorhombic perovskite at 600°C. Lima and Assaf [9] found that the partial substitution of Ni by Fe in the perovskite lattice leads to a decreased reduction temperature of Fe^{3+} ions and the formation of Ni-Fe alloy. In the latter cases, the intercalation of another transition metal (Fe^{3+}, Ni^{3+}…) into the perovskite lattice always leads to modify the catalyst morphology and the catalytic behavior [1,7-10]. In addition, this modification also causes dilution of the transition metal sites and also may affect the reducibility of the parent perovskite.

This article is to report the role of intra-lattice copper in the reduction of cobalt ions in the perovskite lattice. The result may also suggest a simple way to prepare a well-homogenized supported bimetal catalyst system.

2. Experimental Section

2.1 Perovskite preparation

Three nominal formulae of $LaCo_{1-x}Cu_xO_3$ perovskite-type mixed oxides were synthesized by the reactive grinding method [10,11]. In brief, the stoichiometric proportions of commercial lanthanum, copper, and cobalt oxides (99%) were mixed together with three hardened steel balls in a hardened steel crucible (50 mL). Then, the resulting powder was mixed to 50% sodium chloride and further milled for 12 hours before washing the additives with distilled water. The slurry was dried in oven at 60-80°C before calcination at 250°C for 150 min.

A reference sample, $LaCoO_3$ + CuO, was prepared by milling a mixture of the ground perovskite $LaCoO_3$ having a specific surface area of 43 m^2/g with cupric

oxide ($CuO/LaCoO_3$ = 1.5 molar ratio) at ambient temperature before drying at 120°C overnight in oven.

2.2. Characterization

The specific surface area of all obtained samples was measured from nitrogen adsorption equilibrium isotherms at -196 °C measured using an automated gas sorption system (NOVA 2000; Quantachrome). Phase analysis and particle size determination were performed by powder X-ray diffraction (XRD) using a SIEMENS D5000 diffractometer with CuKα radiation (λ = 1.54059 nm). Temperature programmed characterization (TPR) was examined using a multifunctional catalyst testing (RXM-100 from Advanced Scientific Designs, Inc.). Prior to each test analysis, a 50 mg sample was calcined at 500 °C for 90 min under flowing 20% O_2/He (20 ml/min, ramp 5 °C/min). The sample was then cooled down to room temperature under flowing pure He (20 mL/min). TPR of the catalyst was then carried out by ramping under 5 vol% of H_2/Ar (20 mL/min) from room temperature up to 800°C (5 °C/min). The effluent gas was passed through a cold trap (dry ice/ethanol) in order to remove water prior to a thermal conductivity detector (TCD).

3. Results and Discussion

3.1 Physical characteristics

A major drawback of grinding method is usually to produce a low chemical homogeneity and yields a small amount of impurities of unreacted constituent oxides in the final product mixture [2,10]. To investigate the formation of perovskite phase, all perovskite-type mixed oxides are recorded X-ray diffraction. Figure 1 presents XRD patterns for all prepared samples.

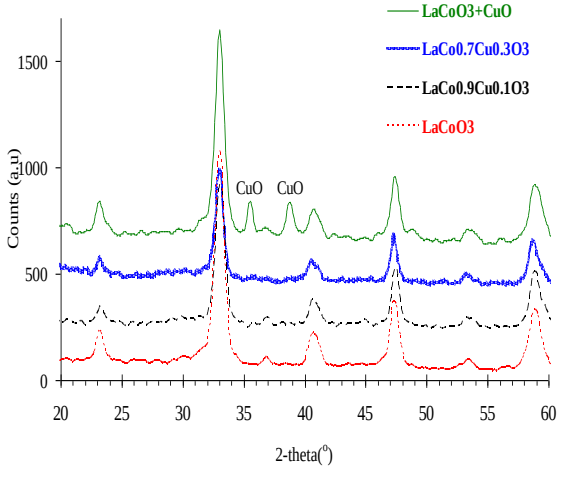

Figure 1. XRD patterns for all ground samples

XRD diffractograms of three perovskites and a mixture of $LaCoO_3$ and CuO are displayed in Figure 1. In general, it is observed that the ground $LaCoO_3$ appears a set of sharp reflection peaks at 23.1, 33.2, 40.6, 47.3, 52.8 and 58.6° representing for the typically crystalline rhombohedral perovskite, in accordance with the JSCDS card Nos. 48-0123, 46-0059, 51-1511) [10, 12,13]. The substitution of Co^{3+} by Cu^{2+} in $LaCo_{1-x}Cu_xO_3$ perovskite mixed oxides is possible up to x = 0.3, and the perovskite is still preserved without changing the crystal symmetry [9,12], substantiated by no observable change in XRD diffractograms between $LaCoO_3$ and $LaCoCuO_3$ patterns. No appearance of other peaks indicates that copper ions are fully incorporated into the perovskite lattice [6,8,9,14]. For the physical mixture, XRD pattern shows the presence of CuO reflected by the appearance of 2-theta values of 35.4 and 38.6° in addition to the $LaCoO_3$ perovskite phase (Fig. 1). In all cases, the reflection lines are rather broadening, implying the formation of nanocrystalites of perovskite [12,13]. The crystal domains of $LaCoO_3$, $LaCo_{0.9}Cu_{0.1}O_3$ and $LaCo_{0.7}Cu_{0.3}O_3$, estimated from the Full Width at Half Maximum (FWHM) of the (102) diffraction peak (2θ = 33.2°) using Scherrer's equation are around 10 nm, in good agreement with SEM observation [6,11,14].

3.2 Morphology and Surface area

Morphological perovskite was examined by SEM technique. Microphotographs of two representative samples are depicted in Figure 2. It is observed a similar surface morphology of SEM micrographs between two selected ground perovskite samples, indicating a high producibility of the grinding synthesis [6,10,11,14]. Moreover, the perovskite powder is constituted by the aggregation of various spherical particles with the average particle size in the range of numerous nanometers, in coincident with the results estimated from Scherrer's equation.

The arrangement of such spherical particles yields many slit-shaped spaces between nanometric particles and thus external surface area increases [11,12,14]. Indeed, the specific surface area of the ground perovskites is in the range of 25 - 56 m^2/g as reported in Table 1 using the BET (Brunauer-Emmet-Teller) equation. The nitrogen adsorption/desorption isotherms are displayed in Figure 3. Adsorption curves of all examined samples are classified into type of II isotherm which is characteristic of a nonporous or possibly micro- and macro-porous material having a high energy of adsorption [15]. However, the isothermal curves are not parallel to the horizontal axis and appears a hysteresis loop at high relative pressure in the narrow range of 0.8-

1.0. This observation may suggest the existence of micropores and some slit-like mesopores in the ground perovskite samples. Indeed, the ground perovskite is consisted of uniform spherical particles [10,14]. There are considerable spaces between the nanometric perovskite grains. As indicated by SEM images, the particles are perfect spheres, the "pore space" or porosity is rather high and the pore sizes are more uniform. The porous structure of the ground perovskite would facilitate the reducibility of transition metal ions in perovskite lattice [12,13].

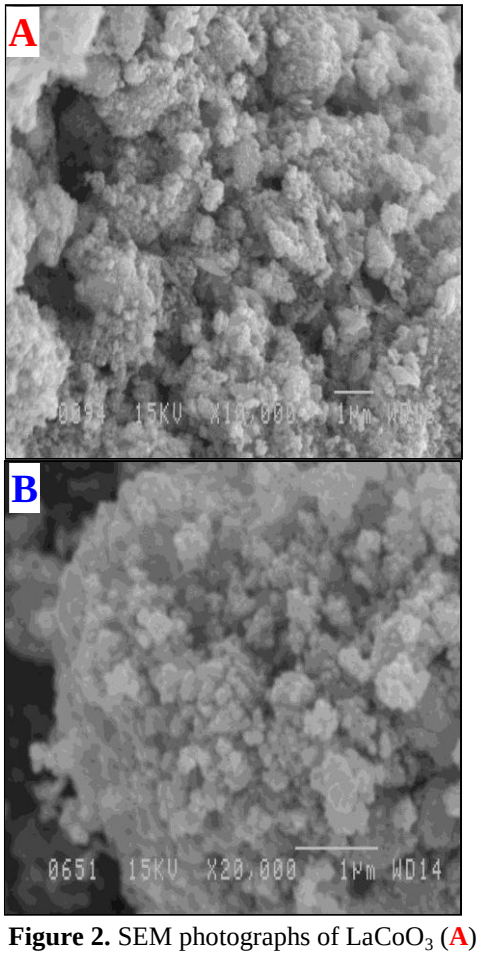

Figure 2. SEM photographs of $LaCoO_3$ (**A**) and $LaCo_{0.9}Cu_{0.1}O_3$ (**B**)

Table 1. Specific surface area of samples

Nominal composition	BET surface area (m^2/g)
$LaCoO_3$	56
$LaCo_{0.9}Cu_{0.1}O_3$	24
$LaCo_{0.7}Cu_{0.3}O_3$	25
$LaCoO_3$ + CuO	21

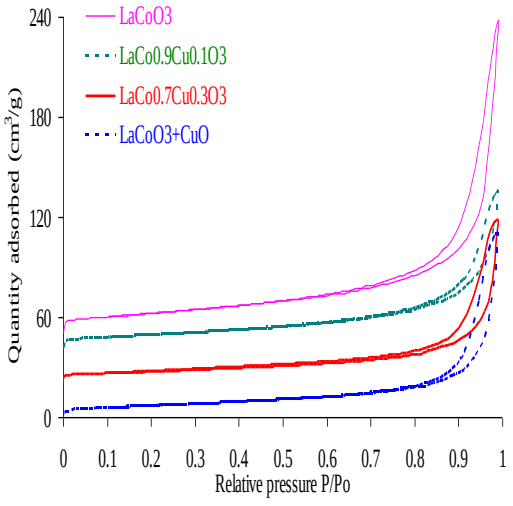

Figure 3. Nitrogen adsorption/desorption isotherms of ground perovskites and reference sample

3.3 Reducibility

The reducibility of the ground perovskites is investigated by the temperature programmed reduction of hydrogen (H_2-TPR). All experiments are carried out from room temperature to 800 °C under H_2/Ar flowrate [12,14,16,17]. Figure 4 represents the variation of TCD signal of hydrogen consumed with reduction temperature.

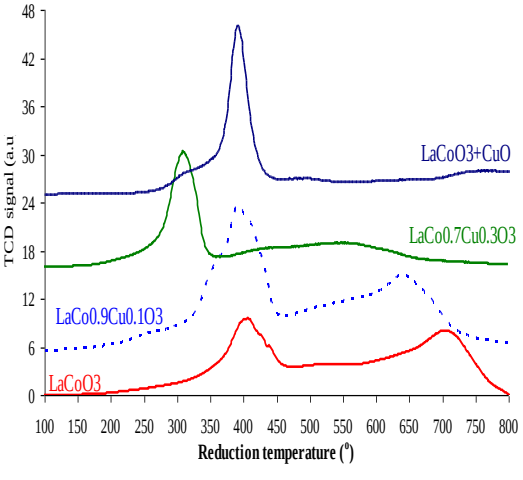

Figure 4. H_2-TPR profiles of ground samples

The reduction of cobaltite perovskites takes place in two consecutive steps as described in Figure 4. H_2-TPR profiles of cobaltite perovskite ($LaCoO_3$) shows two broad bands at 411 and 713 °C. The first peak is attributed to the reduction of Co^{3+} to Co^{2+} in the perovskite lattice [1,2,11,17]. At this step, the perovskite

structure is still remains, evidenced by the XRD patterns collected at different reduction temperatures. As seen in Figure 5, no significant changes in X-ray diffractograms of $LaCoO_3$ are observed in the reduction temperature range of 300-450 ^oC. In the temperature window of 450-500 ^oC, the corresponding XRR patterns of $LaCoO_3$ are essentially unchanged, but the noise to signal ratio dramatically increases, indicating the slightly modification of the perovskite structure at high reduction temperature [16]. This is in good agreement with H_2-TPR result displayed in Figure 4. Furthermore, H_2-TPR signal for the ground $LaCoO_3$ perovskite sample does not reach the baseline after the first reduction step, implying the commencement of second reduction step at 460 ^oC (Fig. 4). Thus, it is suggested that the second step starts at 460 ^oC and lasts through a maximum at 730 ^oC [17,18]. In practice, the XRD pattern of $LaCoO_3$ significantly changes and some new peaks are observed at 550 ^oC, demonstrating the gradual modification in the perovskite structure [2,17,18]. Therefore, this step describes the complete reduction of Co^{2+} to Co^0 accompanied by the gradual destruction of the perovskite structure.

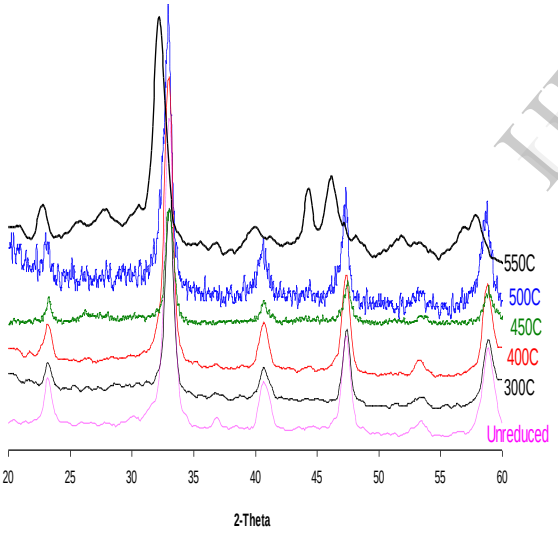

Figure 5. XRD patterns for $LaCoO_3$ reduced at different temperatures in H_2/Ar flowrate

H_2-TPR profiles of $LaCo_{1-x}Cu_xO_3$ perovskites show a slight change in shape as compared with that of cobaltite perovskite. Indeed, H_2-TPR curve of $LaCo_{0.9}Cu_{0.1}O_3$ sample displays a broad peak at lower temperatures along with a visible shoulder at 370^oC. These peaks are ascribed to the reduction of Co^{3+} and Cu^{2+} to lower oxidation states [8,11-13,18]. These signal peaks in $LaCo_{0.9}Cu_{0.1}O_3$ combines into a single peak as increased copper content to x = 0.3 (sample $LaCo_{0.7}Cu_{0.3}O_3$ in Fig. 4). Meanwhile the broad peak at high temperature in the latter sample $LaCo_{0.7}Cu_{0.3}O_3$ becomes more broadening and reaches nearly flat in the range of 400- 650 ^oC. Therefore, it is suggested that the reduction temperatures of both Co^{3+}/Co^{2+} and Co^{2+}/Co^0 in $LaCoCuO_3$ are much lower than those in $LaCoO_3$ (Fig. 1). To demonstrate this hypothesis, we have collected some XRD patterns of a representative sample $LaCo_{0.7}Cu_{0.3}O_3$ reduced at different temperatures [17]. In line with H_2-TPR interpretation, the first reduction step almost terminates at 350 ^oC [19,20] and thus the reduction of $LaCo_{0.7}Co_{0.3}O_3$ at 450 ^oC leads to the deformation of perovskite structure (Fig. 6). This is different from the copper-free perovskite sample ($LaCoO_3$) (Fig. 5) [10,14,15,17]. Moreover, the appearance of week diffraction peaks at 43.6 and 50.6^o is characteristics of metallic copper (JCPDS card No. 04-0836) [11] in addition to the reflection signals of La_2O_3 (JCPDS card No. 74-2430) and Co (JCPDS card 15-0806) and intermediate perovskite phases. These diffraction line intensities increase as increasing reduction temperature to 550^{o}C [2,9].

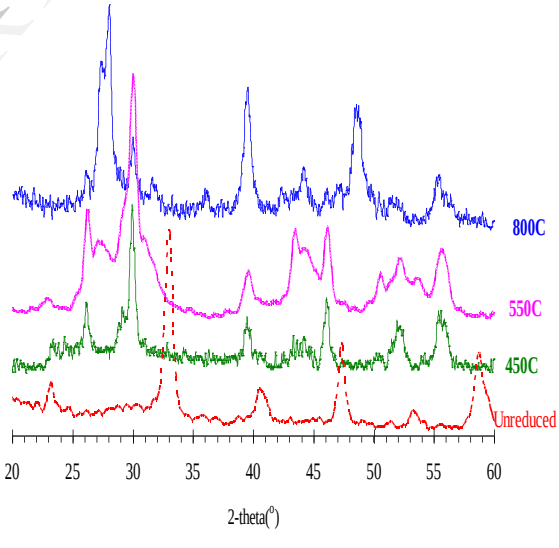

Figure 6. XRD patterns for $LaCo_{0.7}Cu_{0.3}O_3$ reduced at different temperatures in H_2/Ar flowrate

Thus, the presence of copper in the perovskite lattice has strongly promoted the reducibility of cobalt ions in the framework while extra-lattice copper does not significantly affect the reduction ability of cobaltite as analyzed by H_2-TPR traces of CuO/$LaCoO_3$ mixture. The reduction temperatures of Co^{3+} and Cu^{2+} in the blend are almost on par with those in $LaCoO_3$ and single CuO oxide (Fig. 4). The facilitation of intra-lattice copper on the reducibility of cobalt ions in the perovskite lattice is

interpreted by the corresponding extraction of Cu^0 at low temperatures which may act as an active site for dissociation of hydrogen [9,14,18-20]. Therefore, hydrogen molecules chemisorbed on Cu^0 sites who are proximate to cobalt ions. Accordingly, these cobalt ions should be attacked by atomic hydrogen and easily convert to metallic clusters at significantly lower temperatures [9,11,19]. As a consequence, the reduction of $LaCoCuO_3$ leads to the formation of high dispersion of bimetallic copper-cobalt at lower temperatures.

4. Conclusions

Three ground $LaCo_{1-x}Cu_xO_3$ (x = 0 - 0.3) oxides and a blend of $LaCoO_3$ with CuO are prepared by milling method. All $LaCo_{1-x}Cu_xO_3$ samples show well rhombohedral perovskite structure. The perovskite structure is preserved up to x = 0.3. The ground solids are composed of nanometric particles with the average diameter around 10 nm. They possess a moderate surface area and consist of slit-like micro and mesopores. The presence of intra-copper lattice has strongly promoted the reducibility of cobalt in the perovskite framework while extra-lattice copper has negligibly impacted on the thermal stability of $LaCoO_3$ perovskite. All Cu-containing perovskite are reduced at lower temperature as compared with the copper-free perovskite sample and a blend of CuO-$LaCoO_3$.

Acknowledgement. This research is funded by Vietnam National University - Hanoi (VNU) under the Type B of Project, code number QG.12.08.

References

[1] M.A. Pena and J.L.G. Fierro, Chemical structure and performance of Perovskite oxides Chem. Rev. **101**, 1981-2017, 2001.
[2] L.G. Tejuca, J.L.G. Fierro, Properties and applications of perovskite-type oxides, Marcel Dekker Inc., New York, Basel, Hong kong, 1993
[3] M.A. Ulla, R.A. Migone, J.O. Petunchi, and E.A. Lombardo, Surface chemistry and catalytic activity of $La_{1-y}M_xCoO_3$ perovskite (M = Sr or Th), J. Catal. **105**, 107-119, 1987.
[4] S. Ponce, M.A. Pena, J.L.G. Fierro, Surface properties and catalytic performance in methane combustion of Sr-substituted lanthanum maganites, Appl. Catal. B **24**, 193-205, 2000.
[5] T. Arakawa, N. Ohara, J. Shiokawa, Reduction of perovskite oxide $LnCoO_3$ (Ln = La-Eu) in a hydrogen atmosphere, J. Mater. Sci., **21**, 1824-1827, 1986.
[6]. Nguyen Tien Thao, Ho Huu Trung, Vu Nhu Nang, The selective oxidation of styrene over Mg-Co-Al hydrotalcite catalysts, VN J. Chem., **50**(4A) 363-366, 2012.
[7] L. Bedel, A.C. Roger, C. Estournes, A. Kiennemann, Co^0 from partial reduction of $La(Co,Fe)O_3$ perovskites for Fischer-Tropsch synthesis, Catal. Today **85** (2003) 207-218.
[8] S.M., De Lima, , J.M. Assaf, Ni-Fe catalysts based on perovskite-type oxides for dry reforming of methane to syngas, Catal. Lett., **108**, 63-70, 2006.
[9] L. Lisi, G. Bagnasco, P. Ciambelli, S. D. Rossi, P. Porta, G. Russo, and M. Turco, Perovskite-type oxides: II. Redox properties of $LaMn_{1-x}Cu_xO_3$ and $LaCo_{1-x}Cu_xO_3$ and methane catalytic combustion, J. Solid State Chem., **146**, 176-183, 1999.
[10] S. Kaliaguine, A. Van Neste, V. Szabo, J.E. Gallot, M. Bassir, R. Muzychuk, Perovskite-type oxides synthesized by reactive grinding, Appl. Catal. A, **209**, 345-358, 2001.
[11] Nguyen Tien Thao, Effects of alkali additives on the surface properties of $La(Co,Cu)O_3$ perovskites, VN Journal of Chemistry, **50** (5B), 6-10, 2012.
[12] N. Tien-Thao, M. H. Zahedi-Niaki, H. Alamdari, S. Kaliaguine, Effect of alkali additives over nanocrystalline Co-Cu based perovskites as catalysts for higher alcohol synthesis, J. Catal. 245, 348-357, 2007.
[13] L. Armelao, G. Bandoli, D. Barreca, M. Bettinelli, G. Bottaro, and A. Caneschi, Synthesis and characterization of nanophasic $LaCoO_3$ powders, Surf. Inter. Anal., **34**, 112-115, 2002.
[14] R. Zhang, A. Villanueva, H. Alamdari and S. Kaliaguine, Reduction of NO by CO over nanoscale $LaCo_{1-x}Cu_xO_3$ and $LaMn_{1-x}Cu_xO_3$ perovskites, J. Mol. Catal. A **258,** 22-34, 2006.
[15] F. James, B. Condon, Surface Area and Porosity Determinations by Physisorption Measurements and Theory, Elsevier, The Netherlands, pp. 7-15, 2006
[16] E. J. Baran, Structural chemistry and physicochemical properties of Perovskite-like materials, Catal. Today, **8**, 133-151, 1990.
[17] M. Crespin and W.K. Hall, The surface chemistry of some perovskite oxides, J. Catal., **69**, 359-370, 1981.
[18] N. Tien-Thao, M. H. Zahedi-Niaki, H. Alamdari, S. Kaliaguine, Co-Cu metal alloys from $LaCo_{1-x}Cu_xO_3$ perovskites as catalysts for higher alcohol synthesis from syngas, Int. J. Chem. React. Eng. **5**,(A82), 1-16, 2007.
[19] J.A.B. Bourzutschky, N. Homs, and A.T. Bell, Conversion of synthesis gas over $LaMn_{1-x}Cu_xO_{3+\lambda}$ perovskites and related copper catalysts, J. Catal. **124**, 52-72, 1990.
[20] A. Glisenti, A. Galenda, M.M. Natile, Steam reforming and oxidative steam reforming of methanol and ethanol: The behaviour of $LaCo_{0.7}Cu_{0.3}O_3$, Appl. Catal. A, **453**, 102-112, 2013.

*Corresponding author: Nguyen Tien Thao, Ph.D
Department of Petrochemistry, VNU University of Science, Vietnam National University in Hanoi,
19 Le Thanh Tong ST, Hoan Kiem, Hanoi, VIETNAM
Tel.: +84.043.933 1605; Fax.: +84.043.824.1140
Email: ntthao@vnu.edu.vn / nguyentienthao@gmail.com